

Magnetocaloric effect in the high-temperature antiferromagnet YbCoC_2

D. A. Salamatina^{1,2,*}, V. N. Krasnorussky¹, A. V. Semeno^{1,3}, A. V. Bokov¹, A. Velichkov^{2,4}, Z. Surowiec^{2,5}, A. V. Tsvyashchenko¹

1 Vereshchagin Institute for High Pressure Physics, Russian Academy of Sciences, Kaluzhskoe shosse 14, Troitsk, Moscow, Russia

2 Joint Institute for Nuclear Research, 6 Joliot-Curie Str., Dubna, Russia

3 Prokhorov General Physics Institute, Russian Academy of Sciences, 38 Vavilov Str., Moscow, Russia

4 Institute for Nuclear Research and Nuclear Energy, 72 Tsarigradsko shosse Blvd., Sofia, Bulgaria

5 Institute of Physics, M. Curie-Sklodowska University, pl. M. Curie-Sklodowskiej, 1, Lublin, Poland

* dasalam@gmail.com

Abstract

The magnetic H - T phase diagram and magnetocaloric effect in the recently discovered high-temperature heavy-fermion compound YbCoC_2 have been studied. With the increase in the external magnetic field YbCoC_2 experiences the metamagnetic transition and then transition to the ferromagnetic state. The dependencies of magnetic entropy change $-\Delta S_m(T)$ have segments with positive and negative magnetocaloric effects for $\Delta H \leq 6$ T. For $\Delta H = 9$ T magnetocaloric effect becomes positive with a maximum value of $-\Delta S_m(T)$ is 4.1 J / kg K and a refrigerant capacity is 56.6 J / kg.

1 Introduction

Recently, the compounds of GdCoC_2 , GdNiC_2 , NdRhC_2 and PrRhC_2 have been predicted to be topological Weyl semimetals (TWS) [14]. In these compounds, inversion symmetry and time-reversal symmetry are broken due to the noncentrosymmetric orthorhombic structure of the CeNiC_2 -type and low-temperature magnetic transitions, respectively. The unique properties of magnetic TWS can be extremely useful in the context of information technology (e.g., quantum computing), given that such massless charged particles will carry electric current without Joule heating [6]. The theory provides a clear guide to the implementation of magnetic TWS, but so far, there are only a few experimentally confirmed examples of TWS with time-reversal symmetry breaking [3, 9].

The RCoC_2 compounds with magnetic R have ferromagnetic (FM) order at low temperatures [1, 5, 12, 17]. It is believed that in these compounds Co ions do not have a magnetic moment and interactions beyond Ruderman-Kittel-Kasuya-Yosida interaction make a significant contribution to the stabilization of magnetism [16].

One of the promising applications of rare-earth-based magnets is their use as cooling refrigerators. This becomes possible due to their large magnetocaloric effect (MCE).

The MCE effect is the result of a change in the entropy of magnetic spins ΔS_m under the influence of a magnetic field and can be fully characterized by a change in temperature in an adiabatic process (ΔT_m) and a change in magnetic entropy in an isothermal process (ΔS_m) depending on a change in an external magnetic field. ΔS_m can be obtained indirectly from isothermal measurements of the magnetization. Previously, large reversible MCE in HoCoC₂, ErCoC₂ [8], TbCoC₂ [7] and giant reversible MCE in TWS GdCoC₂ [11] have been observed using such measurements.

The moderately heavy fermion compound YbCoC₂ ($\gamma = 190$ mJ/mol-K²) has an antiferromagnetic (AFM) transition at $T_N = 27$ K, which is the highest temperature for the Yb-based magnetic compounds. The magnetic structure of YbCoC₂ in a zero magnetic field at $T = 1.3 - 27$ K is a sine-modulated AFM structure with wave vector $(0, 0, k_z)$, where k_z depends on temperature: $k_z = 0.28$ at T_N and locks-in to the value of $1/4$ below 8 K. The magnetic moment amplitude of Yb ions is $\mu_{Yb} = 1.32 \mu_B$ at 1.3 K, which is lower than the full magnetic moment of a Yb³⁺ free ion ($gJ = 4 \mu_B$) [15].

2 Methods

A polycrystalline single-phase sample of YbCoC₂ was synthesized using high pressure-high temperature technique at $P = 8$ GPa and $T = 1500 - 1700$ K using Toroid high-pressure cell by melting Yb, Co, C and characterized in Ref. [15].

Magnetic moment measurements were made on the VSM option of PPMS, Quantum Design. The isothermal magnetization curves were obtained by increasing the magnetic field from 0 to 9 T and changing the temperature from 2 to 80 K under field cooling conditions with variable temperature steps: $\delta T = 4$ K above and well below T_N and $\delta T = 2$ K near T_N . The magnetic field step was held at $\mu_0 \delta H = 0.1$ T.

3 Results and discussion

Some $M(H)$ dependencies from the temperature range 2 – 80 K are shown on Fig. 1. A detailed analysis of dependencies at $T < T_N$ and in low fields shows that the $M(H)$ curves have almost linear slopes and the magnetization increases with increasing temperature. Also, spontaneous magnetization is absent at all temperatures. This behavior is characteristic of an AFM material. At high magnetic fields ($H \geq H_{c1}$), there is a sharp increase in $M(H)$ associated with a metamagnetic transition. For this transition, hysteresis is observed in the $M(H)$ curves [15] (not shown here). The metamagnetic transition is not observed in the paramagnetic region ($T > T_N$). Therefore, its nature is connected with the AFM structure of Yb magnetic moments.

$M(T)$ measured in magnetic field of 7 T (see Fig. 3) demonstrates a plateau-like behavior at $T \lesssim 24$ K (this temperature is defined as a minimum in dM/dT vs T dependence), which corresponds to the transition from the paramagnetic (PM) to the ferromagnetic state. We have plotted the magnetic H - T phase diagram of YbCoC₂ obtained from the magnetization measurements (see the inset of Fig. 3). H_{c1} and H_{c2} were determined as local maxima in dM/dH vs T and from $M(T)$ dependencies. H_{c1} is associated with the metamagnetic transition to the intermediate magnetic phase (IM), and H_{c2} is probably associated with the transition of YbCoC₂ to the FM state induced by the external magnetic field in which the magnetic unit cell has a finite value of magnetization.

Some Arrot curves have a negative slope (see the inset of Fig. 1). According to the Banerjee criterion [2], this indicates that the metamagnetic transition is of first-order type.

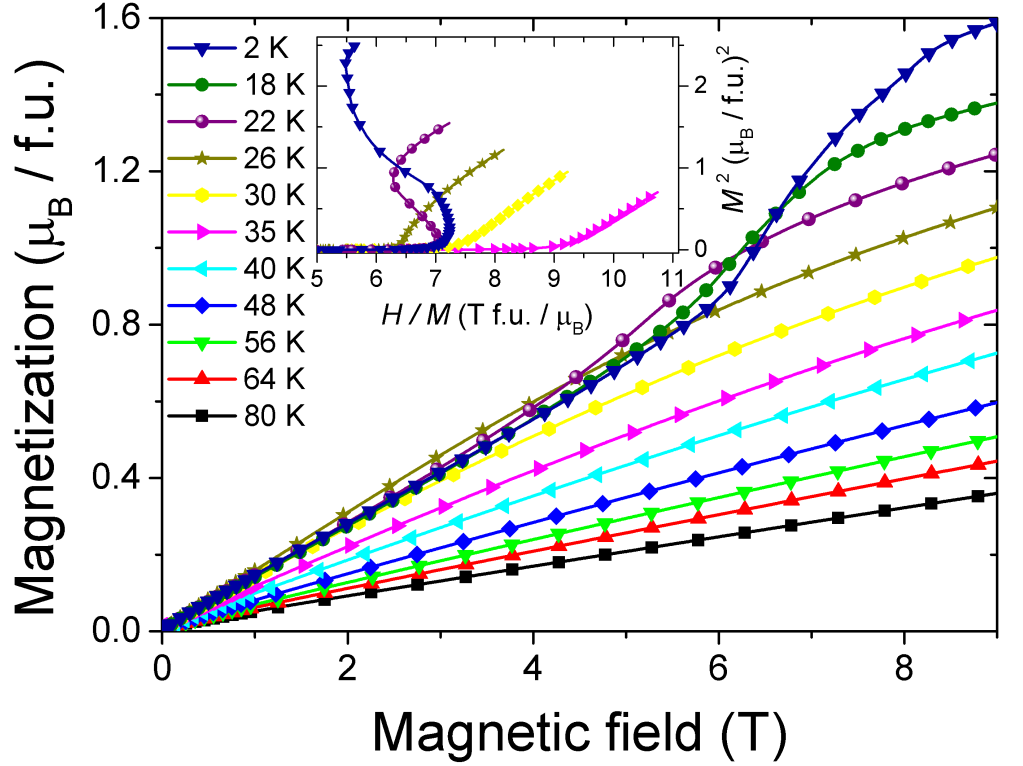


Figure 1. Isothermal magnetization dependencies $M(H)$ of YbCoC_2 . Inset: Arrot plots (M^2 vs H/M) for selected temperatures.

The saturation of magnetization is not observed in fields of 9 T at all temperatures. $M(9 \text{ T}) \approx 35 \text{ J} / \text{T}\cdot\text{kg}$ at $T = 2 \text{ K}$, which corresponds to a magnetic moment of about $1.6 \mu_B / \text{f.u.}$ This value is smaller than the saturation magnetic moment of Yb^{3+} ion ($m_s = 4.0\mu_B$).

It is interesting to note that the mean value of the magnetic moment of the halve positive period of Yb moments sine-wave - the magnetic structure of YbCoC_2 at $T = 2 \text{ K}$ and in zero magnetic field (see Fig. 2), is $1.32 \cdot (1 + 2 \cdot \sin(\pi/4)) / 4 = 0.8 \mu_B / \text{f.u.}$ $M(H)$ at $T = 2 \text{ K}$ reaches this value at H_{c1} . Hence it can be assumed that there is a smooth, almost linear, transformation from the sine-wave modulation to the spin-polarised magnetic structure for $H = 0 - H_{c1}$ with preservation of the Yb mean magnetic moment (see Fig. 2).

As seen from Fig. 1 the $M(H)$ exceeds the value of $0.8 \mu_B / \text{f.u.}$ for $H > H_{c1}$ in the magnetically ordered state. So the mean magnetic moment increases in value above H_{c1} , which may be connected with the increase of Yb mean magnetic moment and the additional contribution from Co.

The temperature dependence of the magnetic susceptibility behaves anomalously at $H = 100 \text{ Oe}$ (not shown). $\chi^{-1}(T)$ decreases slightly above 350 K, similar to the GdCoC_2 compound [10]. It may be connected with the finite value of Co magnetic moment in GdCoC_2 and YbCoC_2 . The finite value of Co magnetic moments in YbCoC_2 was predicted by numerical calculations [15].

$\Delta S_m(T)$ and its relative error for different $\Delta H = H_f - H_i$ were determined from the isothermal magnetizations using well-known numerical methods [13].

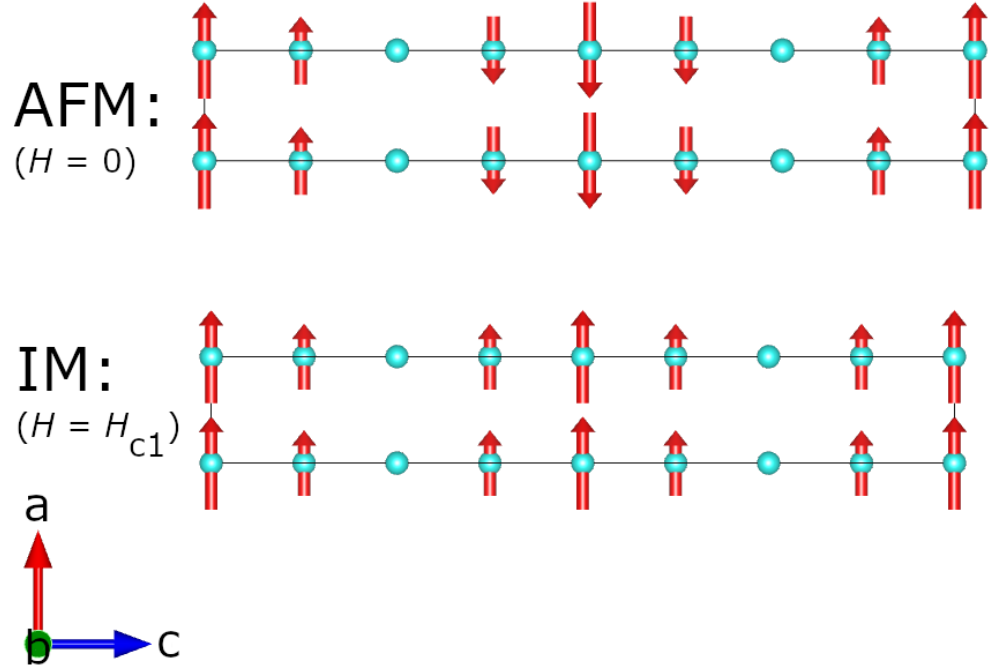


Figure 2. Possible transformation of YbCoC₂ magnetic structure in the external magnetic field: from the antiferromagnetic sine-wave (AFM) at zero field to the intermediate spin-polarised (IM) at $H = H_{c1}$. Only the Yb ions (blue circles) and their magnetic moments (red arrows) are shown.

$$\Delta S_m(T) = \int_{H_i}^{H_f} \left(\frac{\partial M}{\partial T} \right)_H dH, \quad (1)$$

where H_i ($= 0$ in the present case), H_f are the initial and final values of the applied magnetic fields, respectively. The relative error of $\Delta S_m(T)$ did not exceed 10 %.

The dependencies $-\Delta S_m(T)$ for $\Delta H \leq 0 - 6$ T have segments with positive and negative MCE (see Fig. 4). These dependencies have minima, which are connected with the AFM nature of the magnetic ordering in YbCoC₂ in low magnetic fields. The $-\Delta S_m$ minima shift towards lower temperatures with an increase of ΔH in accordance with the phase diagram (the inset of Fig. 3) and the positive MCE appears at $T < 10$ K for $\Delta H \geq 0 - 5$ T. For $\Delta H = 0 - 9$ T a strong external magnetic field suppresses the AFM structure, and MCE becomes positive in the full temperature range and $-\Delta S_m(T)$ has a typical FM "caret-like" shape [4]. $-\Delta S_m(T)$ reaches a maximum of 4.1 J / kg-K at $T \approx 28$ K.

The amount of heat that can be transferred between the cold and hot parts in one cooling cycle is $RC = \int_{T_1}^{T_2} |\Delta S_m| dT = 56.6$ J / kg for $\Delta H = 0 - 9$ T. Here, T_1 , T_2 are the temperatures corresponding to both sides of the half maximum value of $-\Delta S_m(T)$.

If we compare the obtained $-\Delta S_m$ maxima for two TWS, YbCoC₂ and GdCoC₂, we get $\max(-\Delta S_m) / R \ln(2J + 1) = 0.18$ and 0.46, respectively.

4 Conclusion

In conclusion, we have plotted the magnetic H - T phase diagram of YbCoC₂ in the magnetic field range 0–9 T and the temperature range 2–30 K. It is shown that with an

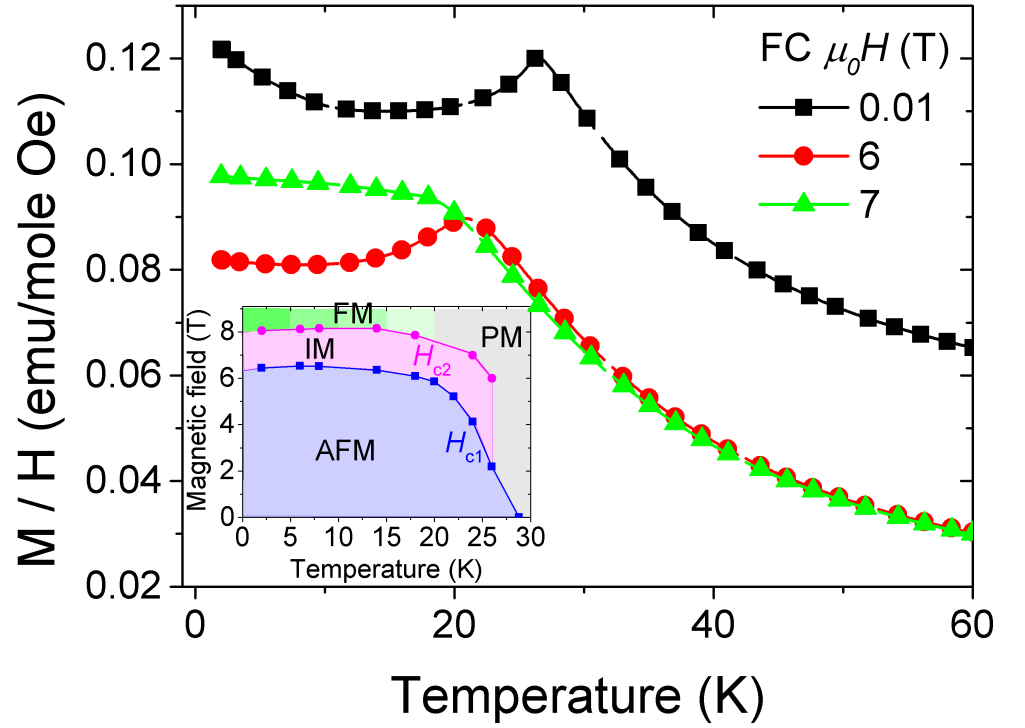


Figure 3. Temperature dependencies of M/H measured in various external magnetic fields in field-cooled mode. Inset: possible magnetic H - T phase diagram of YbCoC_2 (where AFM - antiferromagnetic phase (blue area), IM - intermediate magnetic phase corresponding to the metamagnetic phase transition (pink area) and FM - ferromagnetic phase (green area)).

increase in the external magnetic field, the metamagnetic transition of YbCoC_2 to the IM phase occurs, and with a further increase of magnetic field, it goes to the FM phase. The magnetic structure of the IM and FM phases requires further research by means of neutron diffraction in the external magnetic field and magnetization measurements on single crystal. The smooth transformation from the sine-wave modulation to the spin-polarised magnetic structure for $H = 0 - H_{c1}$ was observed. While further increases in magnetization in higher magnetic field is connected with the increase of Yb mean magnetic moment, and the additional contribution from Co magnetic moments. The MCE for YbCoC_2 has been calculated for ΔH up to 9 T. Due to the AFM - FM transition, MCE in YbCoC_2 changes sign with the increasing of ΔH .

Acknowledgements

The authors are grateful to V. V. Brazhkin for support of the work and M. A. Anisimov for fruitful discussions. This experimental research was funded by the Russian Science Foundation Grant No. 22-12-00008. We are grateful for the support in performing magnetization measurements provided by the Polish representative at the Joint Institute for Nuclear Research.

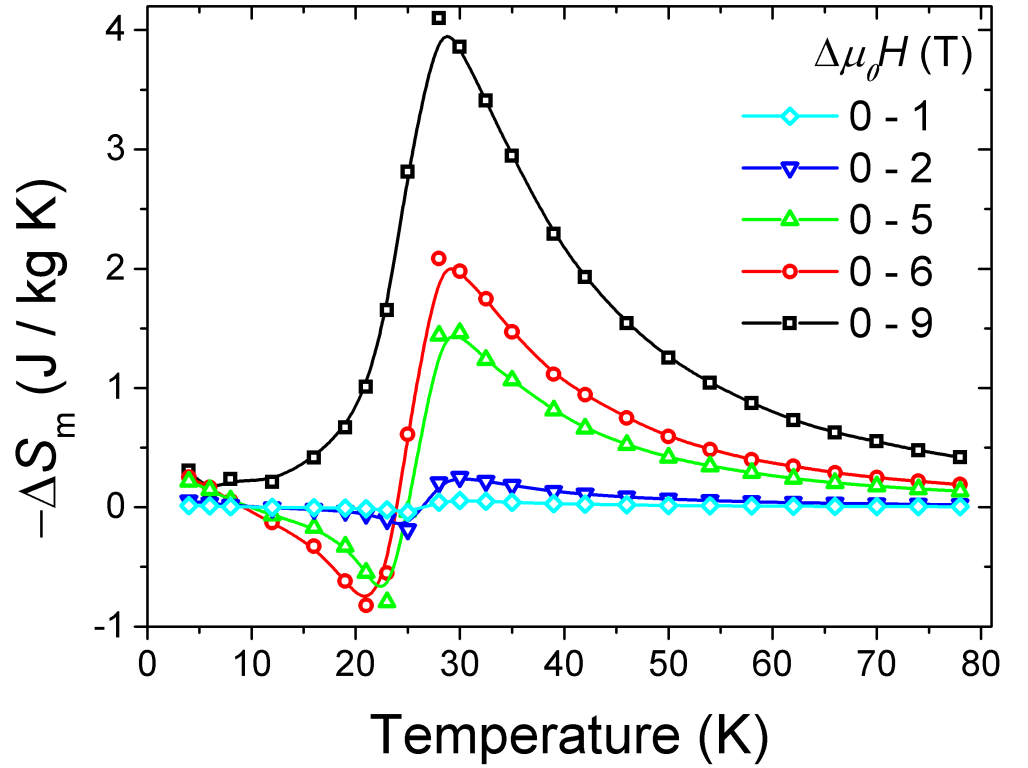


Figure 4. Temperature dependencies of the magnetic entropy change $-\Delta S_m(T)$ for YbCoC_2 for different magnetic field changes (points - experimental data, lines - spline fits).

References

1. H. Amanai, H. Onodera, M. Ohashi, S. Matsuo, H. Yamauchi, Y. Yamaguchi, and N. Sato. Magnetic properties of the ternary carbide DyCoC_2 studied by magnetization measurements, neutron diffraction and ^{161}Dy Mössbauer spectroscopy. *Journal of Magnetism and Magnetic Materials*, 148(3):413 – 418, 1995.
2. B. K. Banerjee. On a generalised approach to first and second order magnetic transitions. *Physics Letters*, 12(1):16–17, 1964.
3. S. Borisenko, D. Evtushinsky, Q. Gibson, A. Yaresko, K. Koepernik, T. Kim, M. Ali, J. van den Brink, M. Hoesch, A. Fedorov, E. Haubold, Y. Kushnirenko, I. Soldatov, R. Schäfer, and R. J. Cava. Time-reversal symmetry breaking type-ii weyl state in YbMnBi_2 . *Nature Communications*, 10(1):3424, Jul 2019.
4. K. A. Gschneidner and V. K. Pecharsky. Magnetocaloric materials. *Annual Review of Materials Research*, 30(1):387–429, 2000.
5. P. A. Kotsanidis, J. K. Yakinthos, and W. Schäfer. Crystal and magnetic structures of RCoC_2 ($\text{R} = \text{Nd, Er, Tm}$). *Journal of Alloys and Compounds*, 242(1):90 – 94, 1996.
6. D. Kurebayashi and K. Nomura. Theory for spin torque in weyl semimetal with magnetic texture. *Scientific Reports*, 9(1):5365, Apr 2019.

7. B. Li, W. J. Hu, X. G. Liu, F. Yang, W. J. Ren, X. G. Zhao, and Z. D. Zhang. Large reversible magnetocaloric effect in TbCoC_2 in low magnetic field. *Applied Physics Letters*, 92(24):242508, 2008.
8. M. Lingjian, J. Youshun, and L. Lingwei. Large reversible magnetocaloric effect in the RECoC_2 ($\text{RE} = \text{Ho}$ and Er) compounds. *Intermetallics*, 85:69–73, 2017.
9. J.-Z. Ma, S. M. Nie, C. J. Yi, J. Jandke, T. Shang, M. Y. Yao, M. Naamneh, L. Q. Yan, Y. Sun, A. Chikina, V. N. Strocov, M. Medarde, M. Song, Y.-M. Xiong, G. Xu, W. Wulfschlegel, J. Mesot, M. Reticcioli, C. Franchini, C. Mudry, M. Müller, Y. G. Shi, T. Qian, H. Ding, and M. Shi. Spin fluctuation induced weyl semimetal state in the paramagnetic phase of EuCd_2As_2 . *Science Advances*, 5(7):eaaw4718, 2019.
10. S. Matsuo, H. Onodera, M. Kosaka, H. Kobayashi, M. Ohashi, H. Yamauchi, and Y. Yamaguchi. Antiferromagnetism of GdCoC_2 and GdNiC_2 intermetallics studied by magnetization measurement and ^{155}Gd Mössbauer spectroscopy. *Journal of Magnetism and Magnetic Materials*, 161:255–264, 1996.
11. L. Meng, C. Xu, Y. Yuan, Y. Qi, S. Zhou, and L. Li. Magnetic properties and giant reversible magnetocaloric effect in GdCoC_2 . *RSC Adv.*, 6:74765–74768, 2016.
12. H. Michor, S. Steiner, A. Schumacher, M. Hembará, V. Levytskyy, V. Babizhetskyy, and B. Kotur. Magnetic properties of HoCoC_2 , HoNiC_2 and their solid solutions. *Journal of Magnetism and Magnetic Materials*, 441:69 – 75, 2017.
13. V. K. Pecharsky and K. A. Gschneidner. Magnetocaloric effect from indirect measurements: Magnetization and heat capacity. *Journal of Applied Physics*, 86(1):565–575, 1999.
14. R. Ray, B. Sadhukhan, M. Richter, J. I. Facio, and J. van den Brink. Tunable chirality of noncentrosymmetric magnetic Weyl semimetals in rare-earth carbides. *npj Quantum Materials*, 7(1):19, Feb 2022.
15. D. A. Salamatina, N. Martin, V. A. Sidorov, N. M. Chitchev, M. V. Magnitskaya, A. E. Petrova, I. P. Zibrov, L. N. Fomicheva, J. Guo, C. Huang, L. Sun, and A. V. Tsvyashchenko. Dualism of the $4f$ electrons and its relation to high-temperature antiferromagnetism in the heavy-fermion compound YbCoC_2 . *Phys. Rev. B*, 101:100406, Mar 2020.
16. W. Schäfer, W. Kockelmann, G. Will, J. K. Yakinthos, and P. A. Kotsanidis. Magnetic structures of rare earths R in RCoC_2 and RNiC_2 compounds. *Journal of Alloys and Compounds*, 250(1):565 – 568, 1997.
17. W. Schäfer, G. Will, P. Kotsanidis, and J. Yakinthos. Magnetic properties of RCoC_2 ($\text{R} = \text{Y}, \text{Gd}, \text{Tb}$) compounds. *Journal of Magnetism and Magnetic Materials*, 88(1):13 – 17, 1990.